A MICROMECHANISTIC INTERPRETATION OF CYCLIC CRACK-GROWTH BEHAVIOR IN A BETA-ANNEALED Ti-6Al-4V ALLOY

Naval Research Laboratory
Washington, D.C.

24 November 1976

NRL Report 8048

A Micromechanistic Interpretation of Cyclic Crack-Growth Behavior in a Beta-Annealed Ti-6Al-4V Alloy

G. R. YODER, L. A. COOLEY, AND T. W. CROOKER

Strength of Metals Branch
Engineering Materials Division

November 24, 1976

NAVAL RESEARCH LABORATORY
Washington, D.C.

SECURITY CLASSIFICATION OF THIS PAGE (When Data Entered)

REPORT DOCUMENTATION PAGE		READ INSTRUCTIONS BEFORE COMPLETING FORM
1. REPORT NUMBER NRL Report 8048	2. GOVT ACCESSION NO.	3. RECIPIENT'S CATALOG NUMBER
4. TITLE (and Subtitle) A MICROMECHANISTIC INTERPRETATION OF CYCLIC CRACK-GROWTH BEHAVIOR IN A BETA-ANNEALED Ti-6Al-4V ALLOY		5. TYPE OF REPORT & PERIOD COVERED Final report on one phase of a continuing NRL Problem. 6. PERFORMING ORG. REPORT NUMBER
7. AUTHOR(s) G. R. Yoder, L. A. Cooley, and T. W. Crooker		8. CONTRACT OR GRANT NUMBER(s)
9. PERFORMING ORGANIZATION NAME AND ADDRESS Naval Research Laboratory Washington, D.C. 20375		10. PROGRAM ELEMENT, PROJECT, TASK AREA & WORK UNIT NUMBERS NRL Problem M01-24 RR 022-01-46
11. CONTROLLING OFFICE NAME AND ADDRESS Chief of Naval Research 800 N. Quincy Street Arlington, VA 22217		12. REPORT DATE November 24, 1976 13. NUMBER OF PAGES 32
14. MONITORING AGENCY NAME & ADDRESS(if different from Controlling Office)		15. SECURITY CLASS. (of this report) Unclassified 15a. DECLASSIFICATION/DOWNGRADING SCHEDULE

16. DISTRIBUTION STATEMENT (of this Report)

Approved for public release; distribution unlimited.

17. DISTRIBUTION STATEMENT (of the abstract entered in Block 20, if different from Report)

18. SUPPLEMENTARY NOTES

19. KEY WORDS (Continue on reverse side if necessary and identify by block number)

Crack bifurcation
Cyclic crack growth
Fatigue crack propagation
Fractography
Structure-sensitive crack growth
Titanium alloys
Widmanstätten microstructure

20. ABSTRACT (Continue on reverse side if necessary and identify by block number)

The cyclic crack-growth resistance of a Ti-6Al-4V-0.20 w/o O alloy, originally mill annealed, is found to be improved significantly through beta annealing. This improvement is particularly pronounced below a transition point in the crack-growth behavior of the beta-annealed material, which occurs at a stress-intensity range Delta K = 23 MPa·$m^{1/2}$. Below this point, the exponent in the growth rate law ($da/dN = C(\text{Delta } K)^m$) changes from approximately 3.1 (above) to 6.3 (below). Consequently, crack-growth rates da/dN below the transition

(Continued)

DD FORM 1 JAN 73 1473 EDITION OF 1 NOV 65 IS OBSOLETE
S/N 0102-014-6601

SECURITY CLASSIFICATION OF THIS PAGE (When Data Entered)

20. Continued

point are reduced by as much as an order of magnitude below the levels determined for the mill-annealed condition at comparable Delta K levels. This reduction is due to crack bifurcation. The transition appears to correlate with the point at which the reversed plastic zone attains the size of the average Widmanstätten packet ($\bar{d}_{wp}$ = 25.4 micrometers). The role of these packets in the bifurcated, structure-sensitive crack propagation observed below the transition is illustrated by metallographic crack-path sectioning. Within individual packets that border the fracture surface, cracks appear to have nucleated at multiple, parallel positions which bear a relation to the orientation of alpha-phase platelets. Electron fractographic evidence also indicates a change from microstructurally sensitive crack growth below the transition to insensitive above. The structure-sensitive growth is faceted in appearance. The facets appear to be comprised of three-superposed features: river-lines reminiscent of cleavage, very fine striations, and a quilted pattern of lines that resembles the Widmanstätten pattern of the microstructure. Evidence is presented that this third feature, which is thought to be associated with the origin of the crack bifurcation, may trace slip bands (and incipient slip band cracks).

CONTENTS

A MICROMECHANISTIC INTERPRETATION OF CYCLIC CRACK-GROWTH BEHAVIOR IN A BETA-ANNEALED Ti-6Al-4V ALLOY

INTRODUCTION

Macroscopic rates of fatigue crack propagation (da/dN) for various alloys are commonly characterized as a function of the stress-intensity factor range ΔK, such that [1]

$$da/dN = C(\Delta K)^m . \quad (1)$$

A logarithmic plot of da/dN vs ΔK over the full spectrum of ΔK levels is typically sigmoidal in form, as shown schematically in Fig. 1 [2]. Region 1 is comprised of low ΔK values in the proximity of the nonpropagating threshold region, while Region 3 is composed of high ΔK levels that approach the fracture toughness. It is the behavior between the inflection points, in Region 2, that is of prime concern to predictions of finite-life structural fatigue. It is this behavior which is most often approximated by Eq. (1) with appropriate values for the parameters C and m.

The work presented herein is part of a larger study to determine whether titanium alloys are amenable to significant enhancement in Region 2 fatigue-crack propagation resistance (FCPR) through heat-treatment/microstructural modification, and if so, to elucidate the mechanisms of such control. This subject is poorly understood [3-5], and the limited data available appear to be in considerable disagreement. Consider, for instance, the results reported in Refs. 6 and 7 as to the influence of a beta anneal (BA) on the Region 2 resistance of Ti-6Al-4V: Ref. 6 reports a fivefold reduction in growth rates relative to those associated with the traditional mill anneal (MA). However, Ref. 7 indicates no effect, even though the reported alloy chemistry and microstructures associated with the MA and BA appear comparable to those given in Ref. 6. Our work indicates that the BA enhances the resistance by up to an order of magnitude, owing mainly to a sharp transition in crack-growth behavior. A micromechanistic interpretation of the transition is offered with supporting metallographic and fractographic evidence.

MATERIAL AND PROCEDURE

The material used was received in the form of 25.4-mm-thick α/β rolled plate with the following composition: Ti-6.7%Al, 4.3%V, 0.10%Fe, 0.20%O, 0.03%C, 0.011%N, and 0.006%H. This alloy was studied in microstructural conditions corresponding to those of the original MA (1 h @ 788°C, air cool) and of a subsequent BA [6] (1/2 h @ 1038°C, cooled @ ≈400°C/h to RT + 2 h @ 732°C, cooled to RT). This heat treatment was performed in a vacuum furnace; cooling was accomplished with a jet of helium to simulate an air-cooling rate. Metallographic samples were etched with Kroll's reagent. Fractographic

Manuscript submitted August 16, 1976.

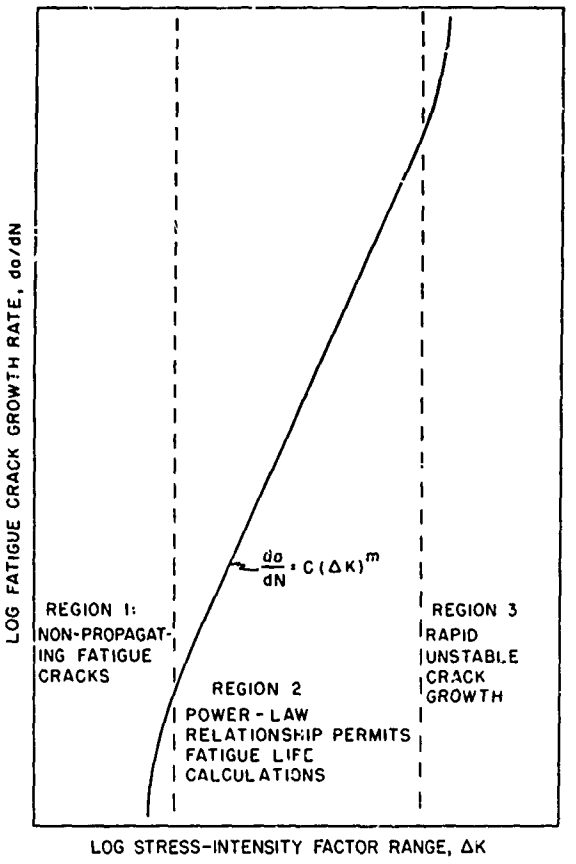

Fig. 1—Schematic of cyclic crack-growth behavior

analyses were made by both scanning electron microscopy and transmission electron microscopy of two-stage, platinum-shadowed, plastic-carbon replicas.

Determinations of growth rates were made from 25.4-mm-thick compact tension specimens with an a/W ratio of 0.486 [8], as shown in Fig. 2. Stress-intensity factors were evaluated according to [8]

$$K_I = \frac{P\sqrt{a}}{BW}\left[30.96 - 195.8\left(\frac{a}{W}\right) + 730.6\left(\frac{a}{W}\right)^2 - 1186.3\left(\frac{a}{W}\right)^3 + 754.6\left(\frac{a}{W}\right)^4\right] \quad (2)$$

where P = load, a = crack length, B = thickness, and W = width (64.8 mm). Specimens were loaded on a 490-kN-capacity, closed-loop hydraulic test machine in ambient laboratory air. For each heat treatment, duplicate specimens were subjected to cyclic tension-to-tension loading with a haversine waveform, at a frequency of 5 Hz and a load ratio of $R = P_{min}/P_{max} = 0.1$. The amplitude of loading was maintained constant throughout the growth rate test of each specimen, but was different for each of the paired specimens so

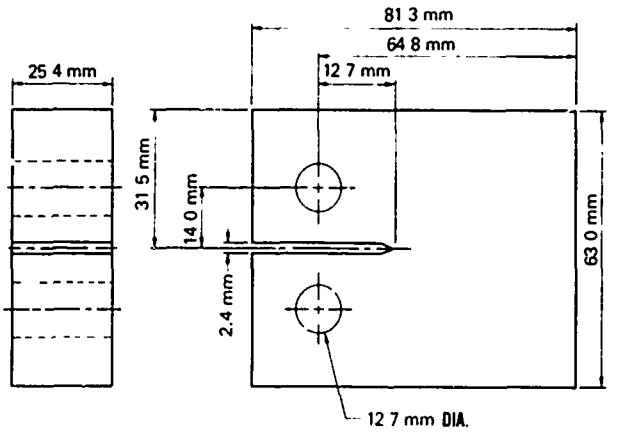

Fig. 2—Compact tension cyclic crack-growth specimen

that da/dN data could be generated over different yet overlapping ranges of ΔK. With the first specimen, rate data were obtained over the range $0.26 \leqslant a/W \leqslant 0.53$, after which the specimen was subjected to a determination of the plane-strain fracture toughness K_{I_c} [9]. With the second specimen, cycled at the higher loading amplitude, rate data were obtained over the range $0.26 \leqslant a/W \leqslant 0.62$. Measurements of crack length were made optically at 15X with a Gaertner traveling microscope. Tensile properties, given in Table 1, were obtained from standard 12.8-mm-diameter specimens of 50.8-mm gage length. Crack-tolerance data are reported for the TL orientation, but tensile properties are given for both the T and L directions [9].

RESULTS AND ANALYSIS

Cyclic Crack-Growth Behavior

Logarithmic plots of da/dN vs stress-intensity factor range ΔK are shown in Fig. 3 for the MA and BA, with the corresponding microstructures. These data indicate much

Table 1—Mechanical Properties

Heat Treatment	Orientation	K_{I_c} (MPa · $m^{1/2}$)	0.2% σ_y (MPa)	σ_{uts} (MPa)	E (GPa)	RA (%)	Elongation (%)	n
Beta Anneal	TL,T	87.4	869	958	117	16	11	0.044
	LT,L	–	892	960	119	23	16	0.036
Mill Anneal	TL,T	41.5	1007	1034	130	29	14	0.021
	LT,L	–	948	986	118	26	15	0.025

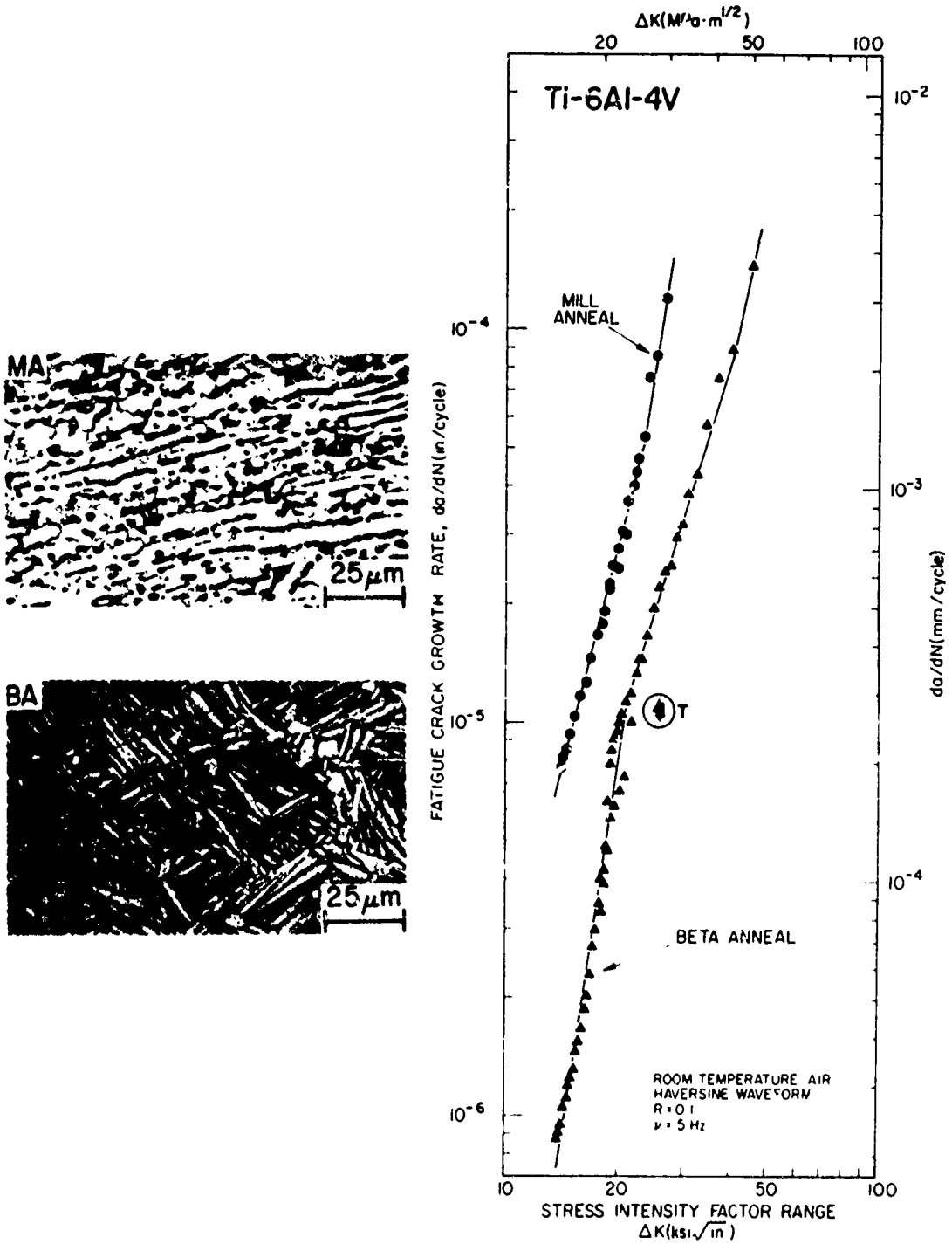

Fig. 3—Microstructures and fatigue crack-growth rates for the mill anneal (MA) and beta anneal (BA)

enhanced resistance associated with the BA, owing primarily to a transition T that occurs at $\Delta K = 23\ MPa \cdot m^{1/2}$. At this point, the exponent in the growth rate law (Eq. (1)) changes from m = 3.1 above to m = 6.3 below. Consequently, growth rates below T are reduced by as much as an order of magnitude from those for the MA. Immediately above T, growth rates are less by about a factor of 3 for the BA. For comparison, the Region 2 exponent for the MA is m = 3.6.

Interpretation of the Transition

The Reversed Plastic-Zone Size vs Microstructural Dimensions—Metallographic and fractographic evidence suggests that T is the point at which the reversed plastic zone, hypothesized by Rice [10] and verified by others [11,12], attains the size of the average Widmanstätten packet ($\bar{d}_{wp}$). The height of the reversed plastic zone above the Mode 1 crack plane can be computed as [10,11]

$$r_y^c = 0.132 \left(\frac{\Delta K}{2\sigma_y^c}\right)^2 \tag{3}$$

where 0.132 is an experimentally validated factor for plane strain [11] and σ_y^c is the cyclic yield stress. For estimation purposes, σ_y^c is commonly approximated by the monotonic yield stress, a practice that the evidence in Refs. 13-15 tends to support for the present case. If σ_y^c is so approximated from Table 1, then at T, r_y^c = 23.4 μm. This value agrees well with measurements of $\bar{d}_{wp}$ = 25.4 μm. This compares to average prior β-grain and α-grain sizes of 142.5 μm and 2.3 μm, respectively. A compilation of quantitative metallographic data for the MA and BA is shown in Table 2. (If in the case of the MA a transition to structure-sensitive behavior were to be predicted based on $\bar{d}_\alpha$, it would be expected to occur at a lower level of ΔK than for the data reported in Fig. 3.)

Structure-Sensitive vs Structure-Insensitive Growth—If such a critical r_y^c is associated with T, a change in the micromode of crack growth should occur, from microstructurally sensitive below T to insensitive above. Electron fractographic evidence supports such a change: The morphological similarities of the fracture surface topography illustrated in Fig. 4a and the microstructure shown in Fig. 3 indicate the structure-sensitive nature of crack propagation below T. By contrast, above T the fracture topography appears to be structure insensitive, consisting primarily of broad, relatively flat areas covered with striations (Fig. 4b). (It might be, however, that the normal striation mode will fail to reveal certain types of structural dependence, such as those owing to texture.)

Table 2—Quantitative Metallographic Data

Heat Treatment	$\bar{d}_\alpha$ (Avg. α-Grain Size)	$\bar{d}_\beta$ (Avg. Prior β-Grain Size)	$\bar{d}_{wp}$ (Avg. Widmanstätten Packet Size)
BA	2.3 μm	142.5 μm	25.4 μm
MA	4.8 μm	–	–

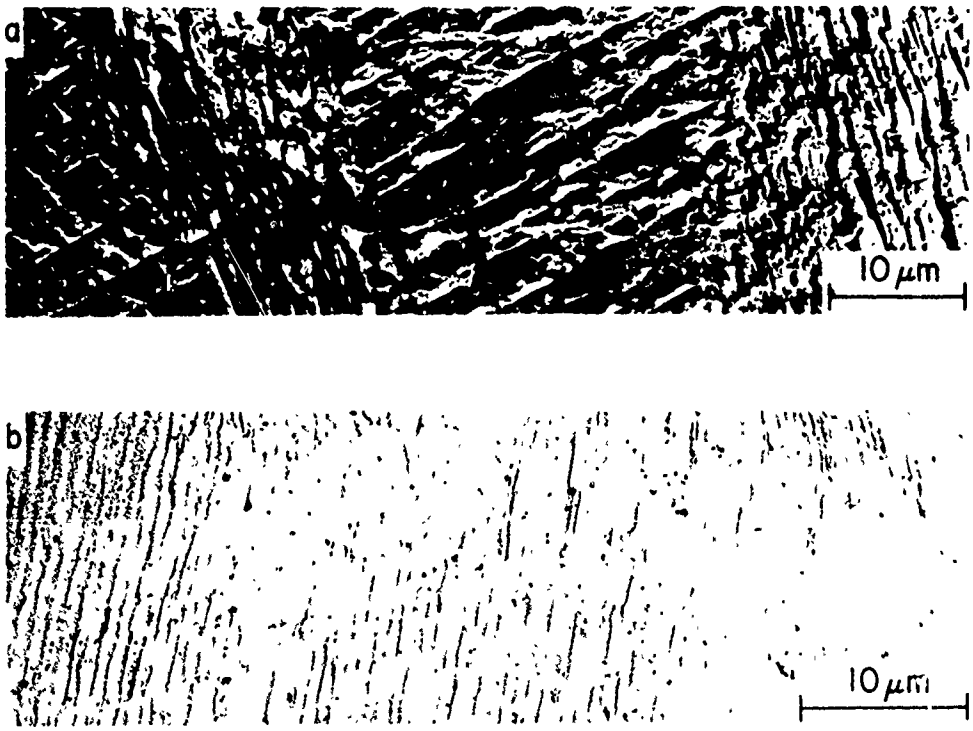

Fig. 4—Replica electron fractographs for the BA: (a) Below T, $\Delta K = 17.1$ MPa · $m^{1/2}$; (b) above T, $\Delta K = 30.8$ MPa · $m^{1/2}$

Crack Bifurcation in the Widmanstätten Packet—The importance of the Widmanstätten packet to the structure-sensitive nature of crack propagation below T is further indicated by crack-path sectioning results. In individual packets that border the fracture surface, cracks appear to have nucleated at multiple, parallel positions that bear a distinct relation to the orientation of α-phase platelets, as shown in Fig. 5. This suggests crystallographic cracking, as though individual parallel platelets behaved in unison, as a single crystal. This is reasonable, because a parallel set of platelets that transform from the β-phase according to the Burgers relation [16,17]:

$$\{110\}_\beta // (0001)_\alpha ,$$

$$\langle 111\rangle_\beta // \langle 11\bar{2}0\rangle_\alpha$$

(of which there are several variants) is of a single orientation [18].

The significantly enhanced resistance observed below T in Fig. 3 is directly attributable to this crack bifurcation,* which reduces the effective ΔK (and therefore da/dN)

*Since the commencement of this writing, cyclic crack growth similar to that in Fig. 5 has been brought to the authors' attention [19] for another β-annealed titanium alloy, IMI 685. In that work, it was observed that cracks within a Widmanstätten packet exhibited a similar relation to the orientation of the α phase platelets as displayed in Fig. 6, rather than running parallel to the α β interfaces. It was further observed that, with slower cooling rates from the β-phase field, and the consequent increase in d_{wp}, the enhancement in crack propagation resistance was greater.

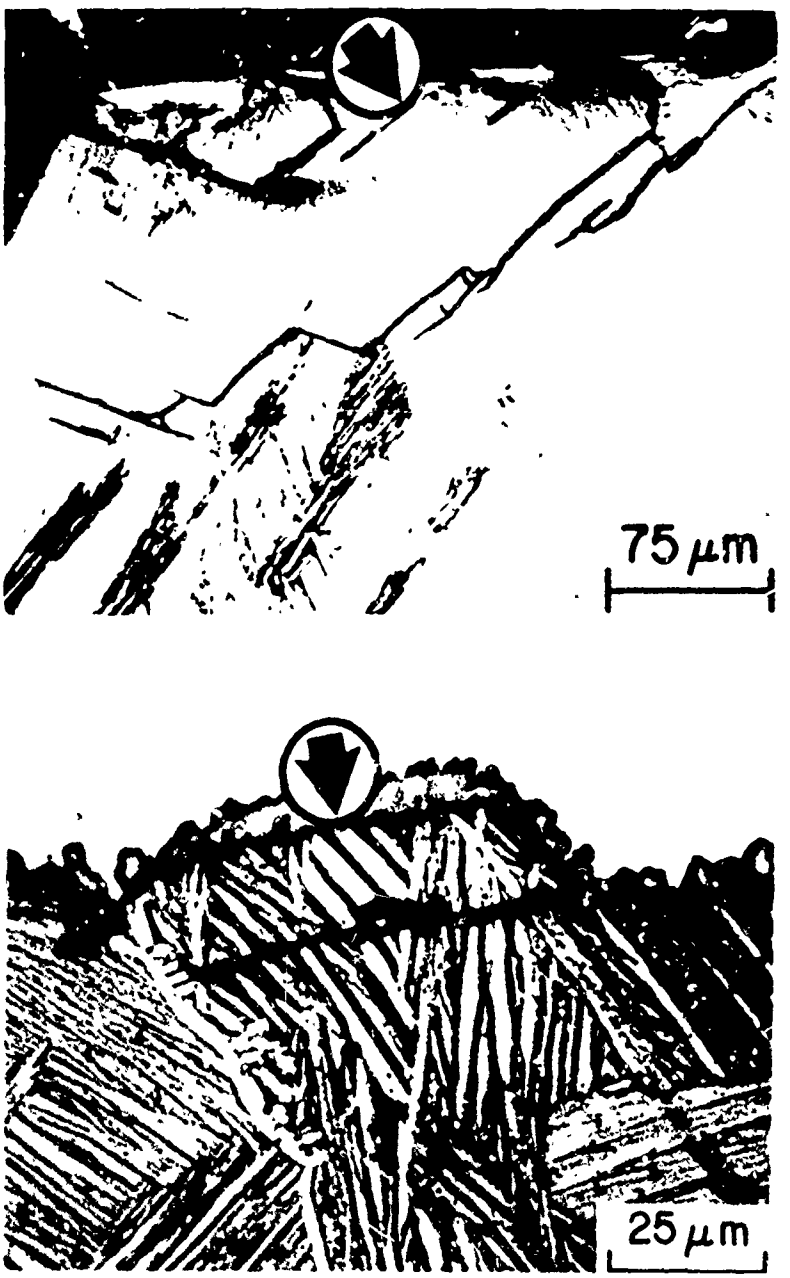

Fig. 5—Metallographic crack path section for the BA: (a) ΔK = 17.4 MPa · $m^{1/2}$; (b) ΔK = 18.5 MPa · $m^{1/2}$. Arrow indicates trace of fracture surface (Cu, Ni-plated).

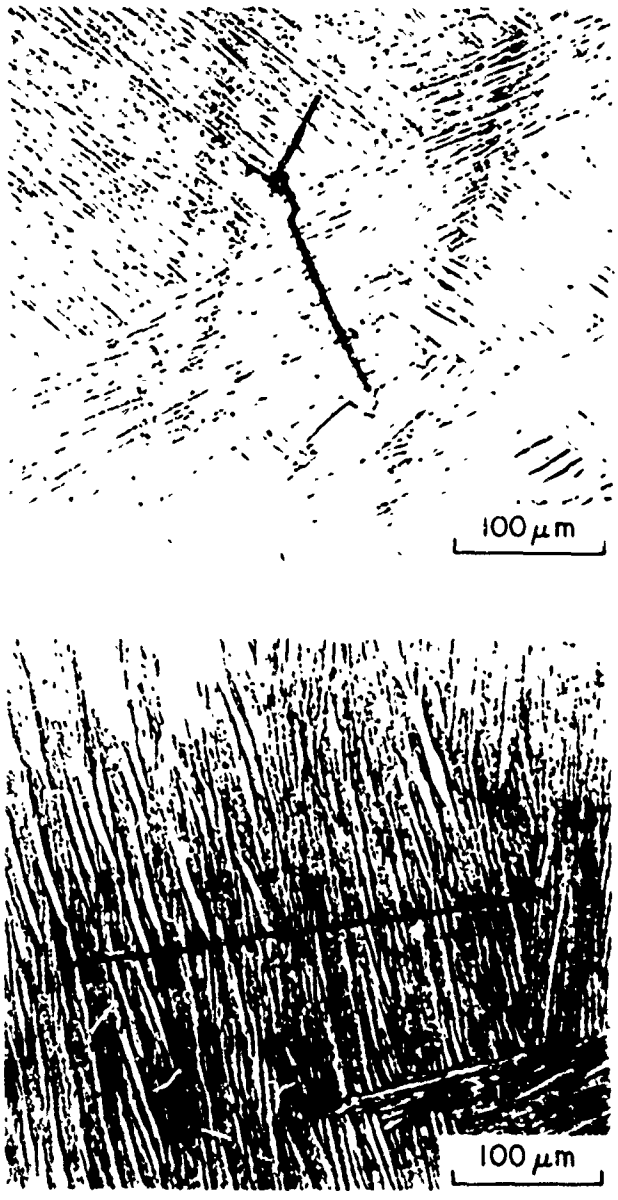

Fig. 6—Crystallographic cracking of Widmanstätten packets of another titanium alloy (IMI-685) subjected to cyclic crack growth (courtesy P. A. Blenkinsop [19])

by dispersing the strain-field energy of the macroscopic crack among multiple crack tips. Such an effect has previously been reported for cyclic crack growth in pearlitic steels [20].

Evidence of the bifurcation comparable to that exhibited in Fig. 7a was also witnessed at the specimen surfaces during growth rate testing. For the MA, by contrast, the crack path was straight and collinear with the trace of the Mode 1 crack plane, as illustrated in Fig. 7b.

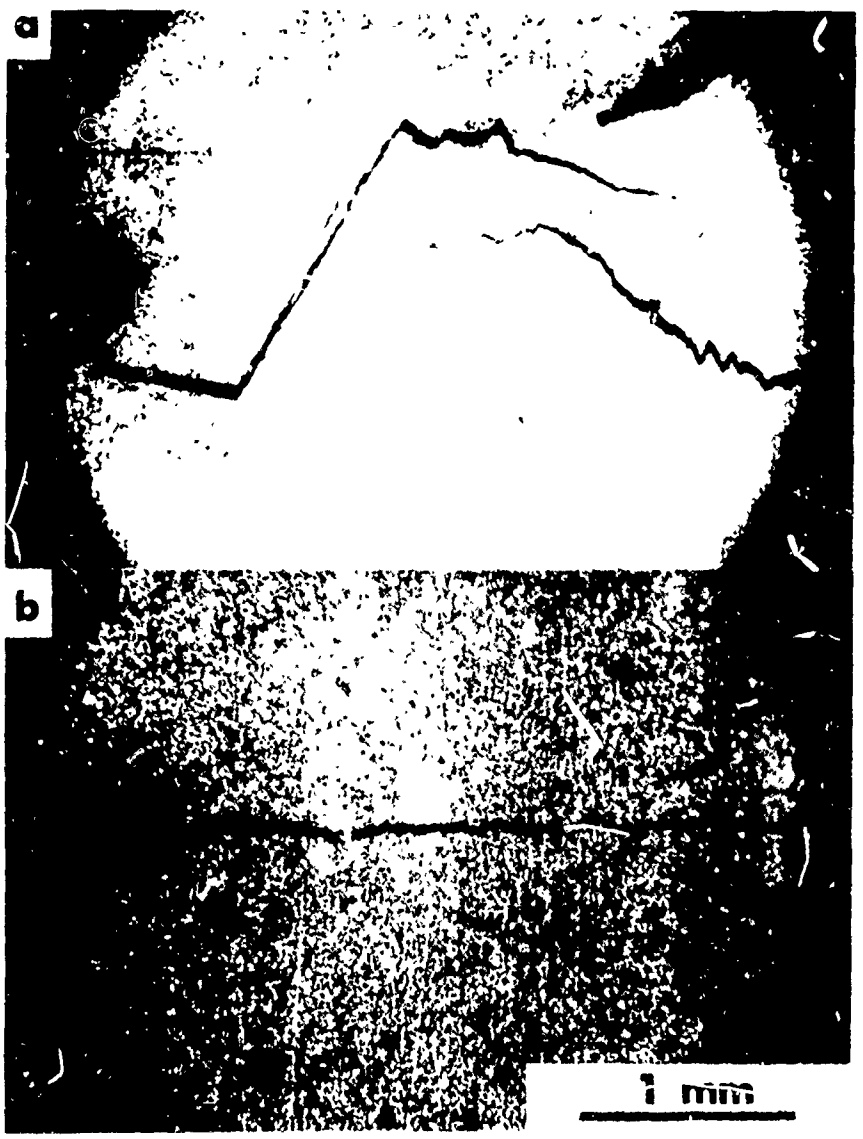

Fig. 7—(a) Example of bifurcation observed at specimen surface in the cyclic crack growth of a Widmanstätten Ti-6Al-4V alloy, relative to (b) a normal nonbifurcated crack in a titanium alloy

Observations on the Overall Enhancement

Over the full range of ΔK levels examined for the BA and MA, the enhancement in crack-growth resistance with the BA is significant. Besides the transition T, there are two other notable features in Fig. 3 that distinguish the enhancement:

(a) The onset of accelerated Region 3 growth rates is displaced to a much higher ΔK level for the BA (from $\approx$25 MPa$\cdot m^{1/2}$ for the MA to $\approx$40 MPa$\cdot m^{1/2}$). For plane-strain conditions, the ΔK level associated with the onset is related to fracture toughness, and for lesser constraint to a critical level of crack-opening displacement [2]. In the present work, the maximum K levels associated with the respective onsets represent full plane-strain constraint, as defined by the specimen size requirements of ASTM E399-74. Consequently, it is not surprising that the ratio of onset levels is in roughly the same proportion as the K_{Ic} levels reported in Table 1 (41.5 MPa$\cdot m^{1/2}$ for the MA and 87.4 MPa$\cdot m^{1/2}$ for the BA).

(b) For Region 2 behavior, there is a substantial offset (to the right in Fig. 3) for the BA data *above* T relative to those for the MA. Put another way, the growth rates for the MA substantially exceed those for the BA above T (or any extrapolation of that portion of the BA data trend in Fig. 3 to ΔK levels below T). As noted earlier, for the BA above T, cyclic crack growth occurred predominantly in the normal striation mode (cf. Fig. 4b). For the MA, in contrast, the cleavagelike mode evident in Fig. 8 appears to cover about 50% of the fatigue fracture surface, with the normal striation mode accounting for the remainder. These cleavagelike features are superposed with striations, in accord with the case described in Ref. 21. Though such "cyclic cleavage" is to be distinguished from "static-mode cleavage,"* described in Refs. 22-24 as a micromechanism of cyclic crack growth, the results for the MA suggest that the incidence of "cyclic cleavage," without concurrent crack bifurcation, may reduce crack-growth resistance. If so, these results would be consistent with the observation in Ref. 22 that growth rates are accelerated as the proportion of static-mode cleavage increases relative to the normal striation mode. On the other hand, the evidence in Ref. 21 does not indicate the propagation resistance associated with cyclic cleavage to be inferior to that associated with the normal striation mode. (No mention is made in Ref. 21 of crack bifurcation associated with the appearance of cyclic cleavage.) Perhaps, then, the inferior resistance for the MA is attributable to the much smaller monotonic strain hardening exponent n noted in Table 1† (0.021 vs 0.044 for the BA) or the somewhat greater yield strength (1007 vs 869 MPa for the BA).

Further Observations on the Nature of Structure-Sensitive Growth

Because of the importance of the structure-sensitive mode of cyclic crack growth in the case of the BA, it is appropriate to further examine its origins. As shown by the scanning electron micrographs in Figs. 9 and 10, the fracture surface is faceted in appearance.

*For example, the former mode is reported to be ΔK dependent [21], the latter K_{max}-dependent [22].
†Values of n were computed according to [25]

$$(0.002\, e/n)^n = \sigma_y/\sigma_{uts} \qquad (4)$$

where e is the natural logarithmic base (2.718).

Fig. 8—Cyclic cleavagelike features and striations in the fracture surface for the MA at $\Delta K = 17.5$ MPa · $m^{1/2}$. Replica electron fractograph.

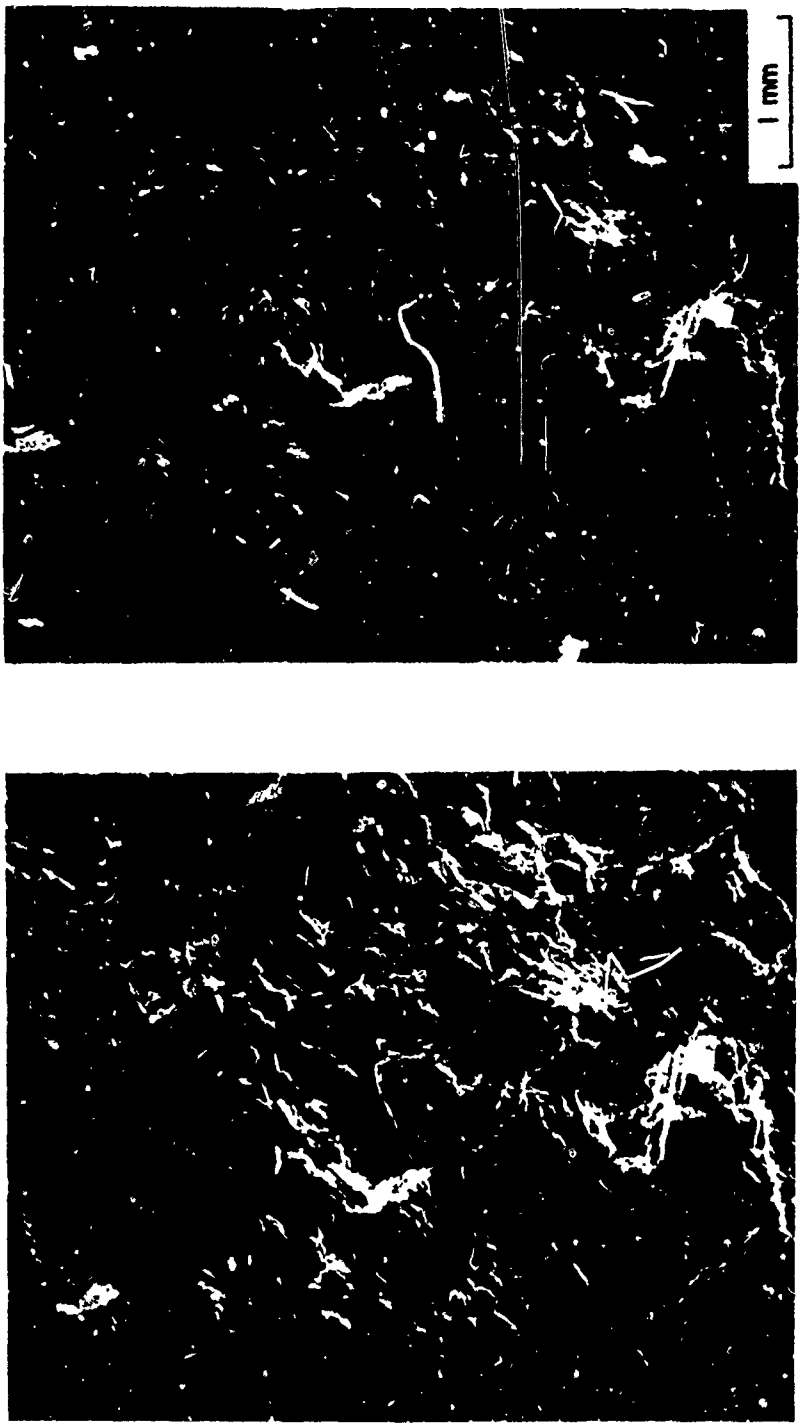

Fig. 9—Faceted morphology of structure-sensitive crack growth for the BA at $\Delta K = 18 \pm 2$ MPa · m$^{1/2}$. Scanning electron fractographs (stereo pair).

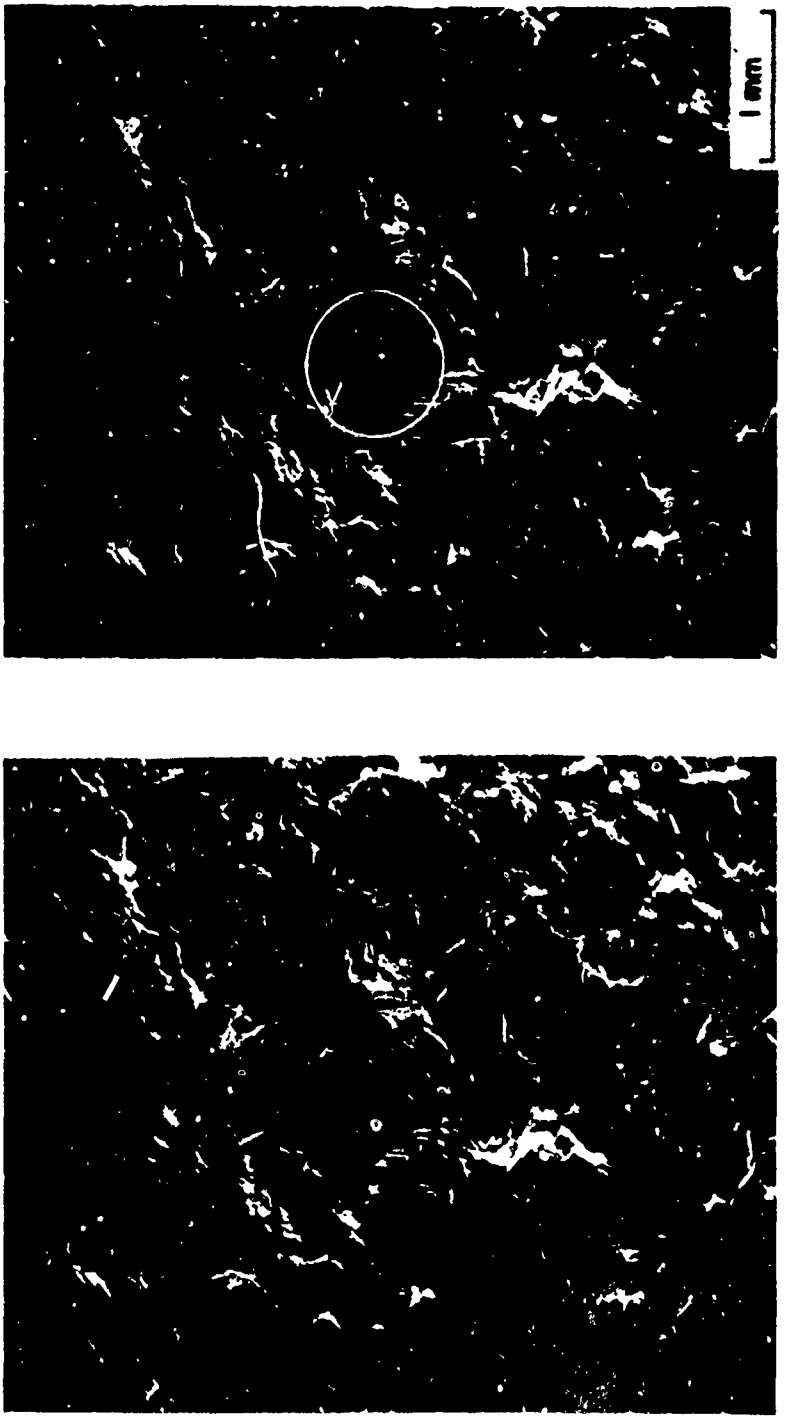

(a) stereo pair of scanning electron micrographs (SEM) at 20X.

Fig. 10—Detail of faceted morphology for the BA below T.

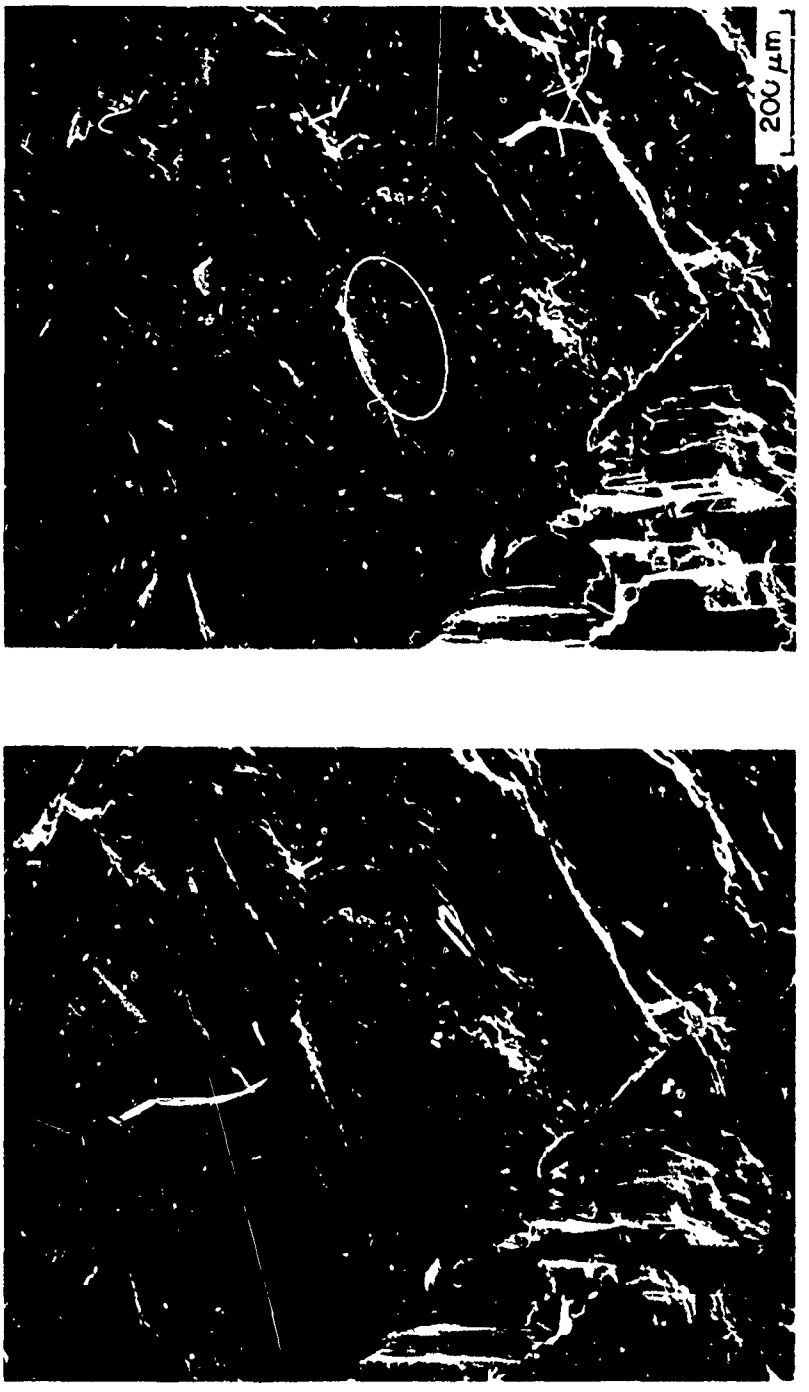

Fig. 10b—Detail of circled region of Fig. 10a at 95X; stereo pair of SEM

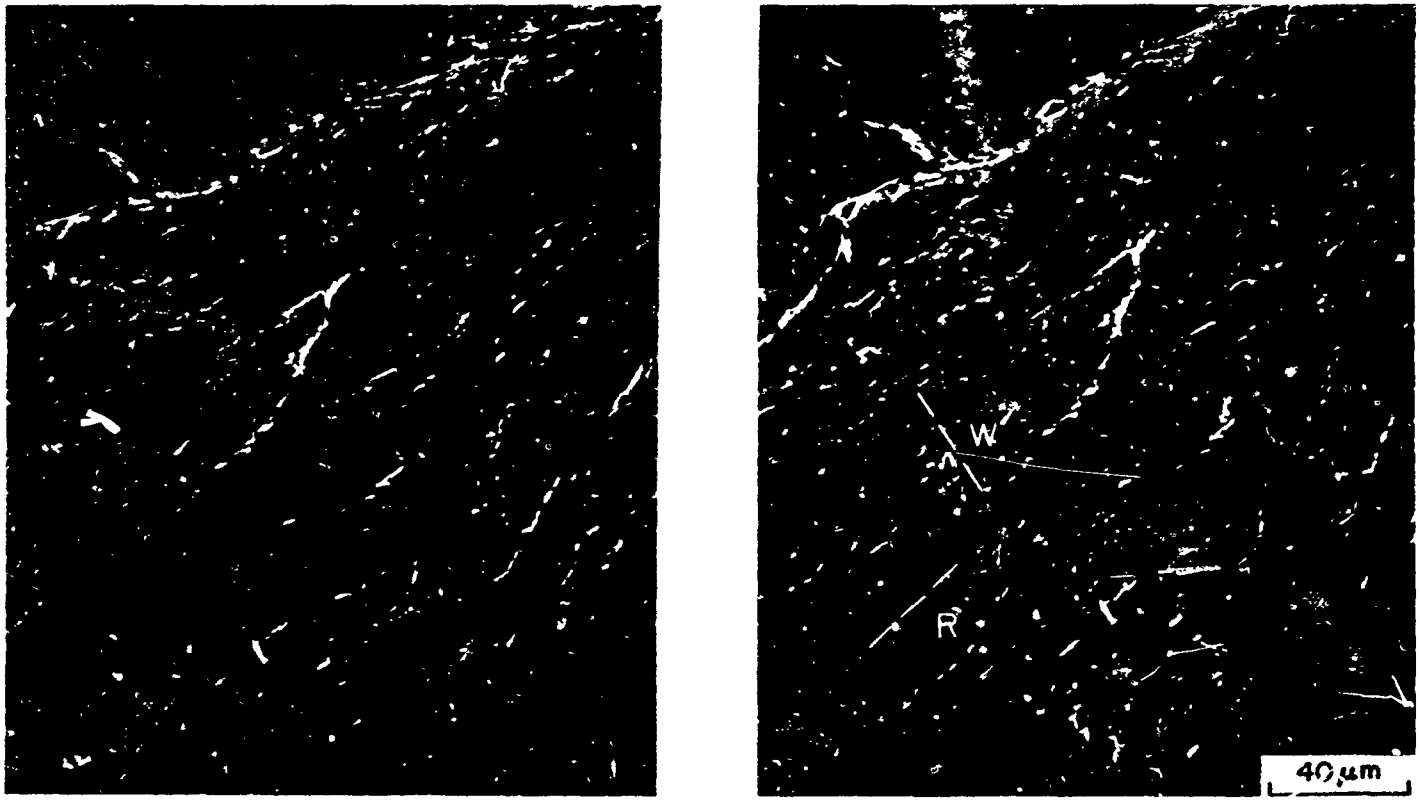

Fig. 10c—Detail of circled region of Fig. 10b at 475X (W-lines and R-lines are indicated with arrows); stereo pair of SEM

Fig. 10d—Detail of faceted morphology of the BA below T showing fine striations on facet at 14,650X; replica electron fractograph

A recent comprehensive study [26] reveals that such a faceted morphology occurs at relatively low ΔK levels in a broad spectrum of alloys with close-packed crystal structures; this morphology has been attributed to a glide plane decohesion mechanism [26,27].

Examination of the facets by both replica and scanning electron fractography, over a wide range of magnifications, discloses the complexity of their nature; they exhibit three different types of superposed lineal features:

1. The river-line patterns reminiscent of cleavage (hereafter referred to as "R-lines"), exhibited in Figs. 9-11 (Figs. 10c and 11 especially)

2. The quilted pattern of lines displayed in Fig. 4a which resembles the Widmanstätten microstructure and perhaps plays a key role in the structure-sensitive crack growth. These lines, hereafter referred to as "W-lines," are also indicated in Figs. 10b, 10c, and 11.

3. Striations,* the characteristic mode of fatigue crack propagation, as evidenced in Figs. 10d and 12. Striation spacings λ are in quite reasonable agreement with the macroscopic growth rate data of Fig. 3. For example, Fig. 12 indicates that $\lambda \approx 5.7 \times 10^{-5}$ mm (570 Å), which compares to $da/dN \approx 4 \times 10^{-5}$ mm/cycle for $\Delta K = 17.1$ MPa$\cdot$m$^{1/2}$ in Fig. 3.

The following observations are relevant to interpretation of the W-lines:

1. They are not to be confused with striations, as they are ≈2 orders of magnitude larger.

2. The R-lines are thought to be associated with α/β interfaces [28,29]; thus, it seems likely that W-lines are not, as their orientation is closer to normal than parallel to the R-lines, as shown in Figs. 10c and 11. In fact, a similar orientation between the multiple, parallel cracks in Fig. 5 and the α/β interfaces is observed.

3. Multiple, parallel cracks appear to open along the W-lines, as shown in Fig. 13.

4. The W-lines are of a similar configuration to that defined by the α/β interfaces of the Widmanstätten microstructure in Fig. 3.

5. Note that the W-lines in Fig. 13 are not perfectly straight and parallel but rather are curved and intersecting in some cases.

6. Figure 14 shows large offsets in R-lines where they are crossed by W-lines.

Observations 2 and 6 strongly suggest that W-lines trace slip bands (and ensuing slip-band cracks). Furthermore, in view of Observations 2, 3, and 6, it is conceivable that the multiple, parallel cracks that describe the crystallographic bifurcation in Fig. 5 may also be traces of W lines. The other observations are not inconsistent with such an interpretation.

*It should be noted that the superposition of very fine striations on these facets is in accord with the findings in Ref. 21, where fine striations were reportedly superposed on cleavage facets in the cyclic crack growth of a Ti-6Al-4V alloy. In Ref. 26, however, no such superposed striations were reported in the faceted, cyclic crack growth of the several alloys investigated, including a Ti-6Al-4V alloy.

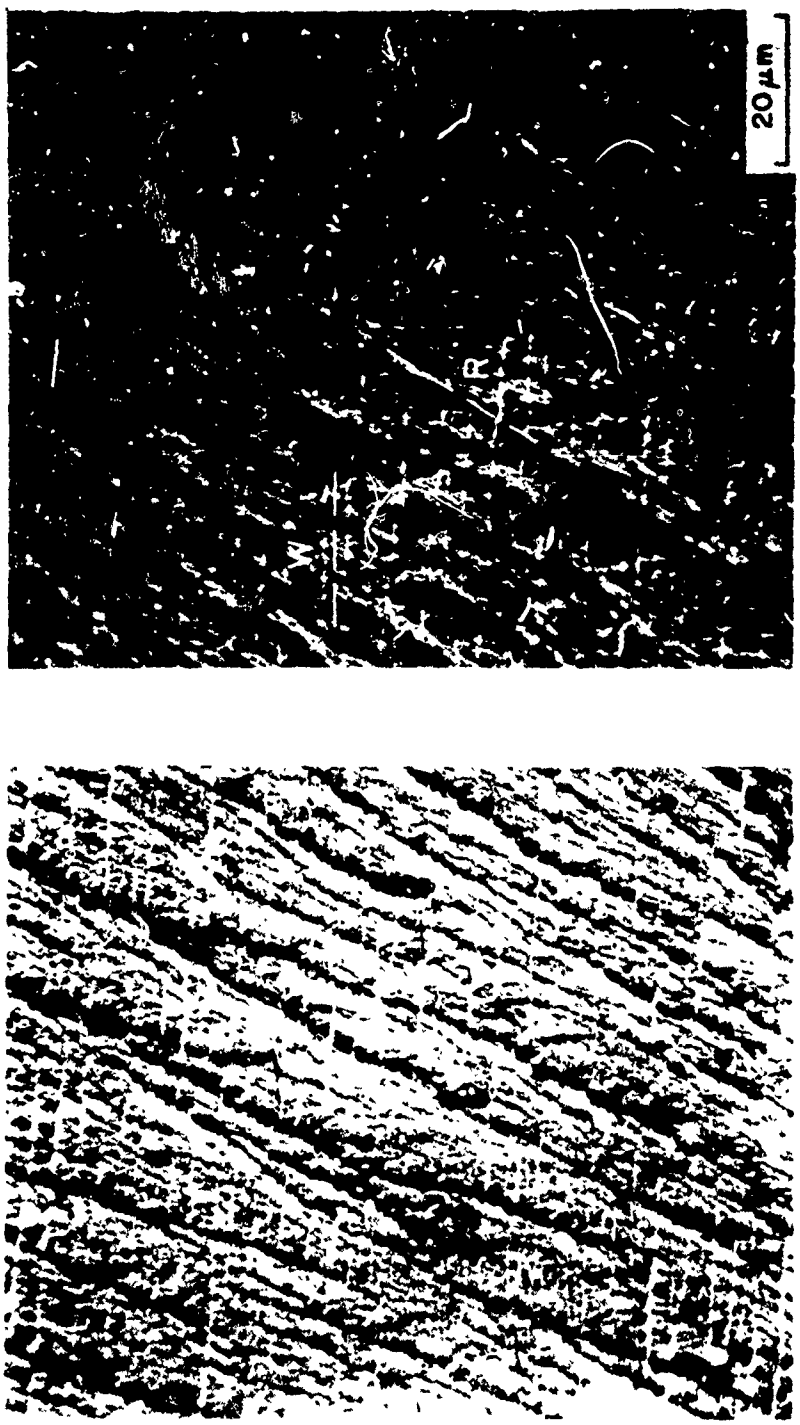

Fig. 11—R-lines and W-lines in the structure-sensitive cyclic crack growth for the BA below T. Scanning electron fractographs (stereo pair).

Fig. 12—Fine striations in the structure-sensitive crack growth for the BA, $\Delta K = 17.1\ MFa \cdot m^{1/2}$. Replica electron fractograph.

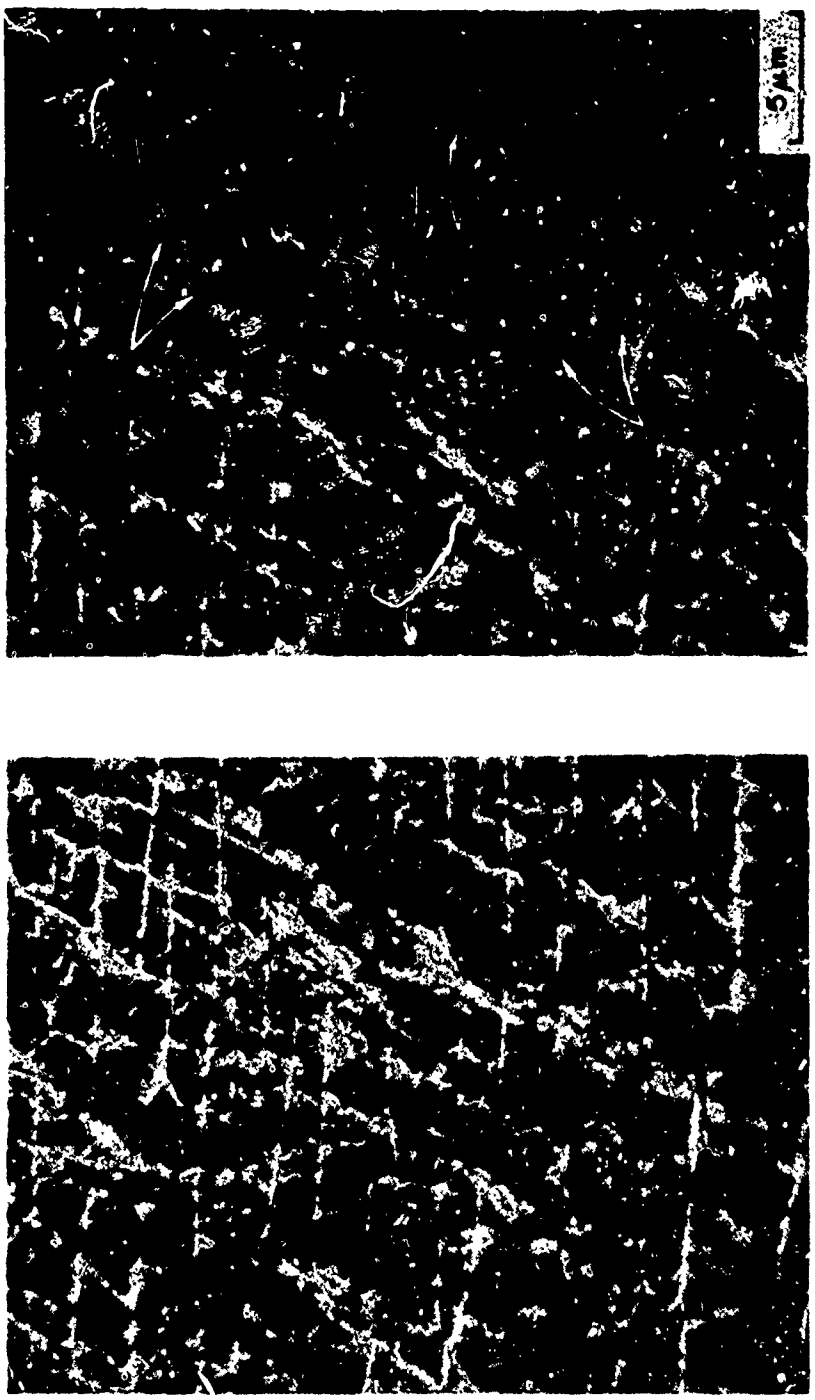

Fig. 13—W-lines and associated fine cracks (arrows) in the faceted crack growth for the BA below T. Scanning electron fractographs (stereo pair).

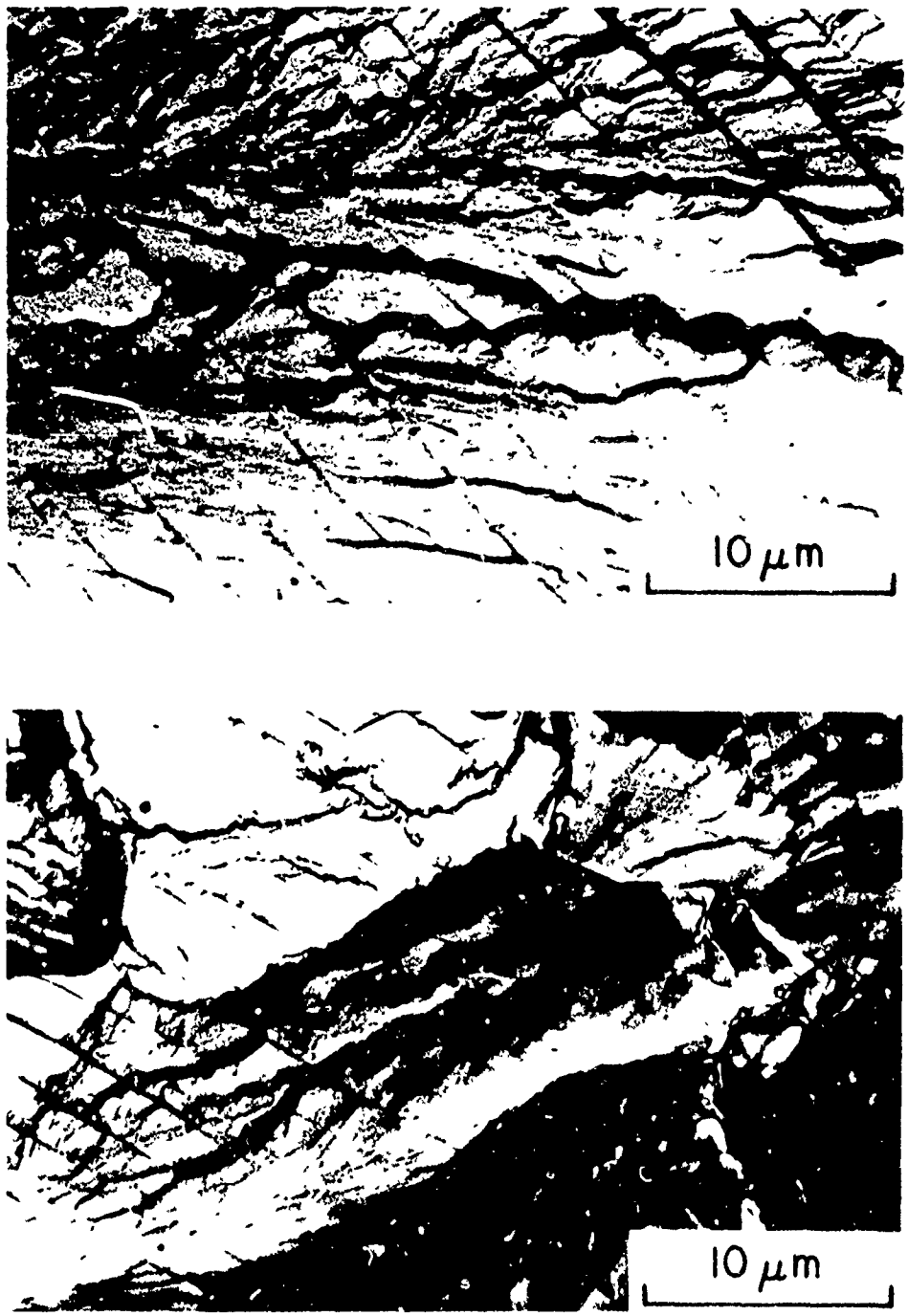

Fig. 14—Structure-sensitive cyclic crack growth for the BA below T. Note offsets in R-lines at junctures with W-lines. Replica electron fractographs.

(It is also pertinent to note that in Ref. 26, slip-band cracking was associated with the faceted behavior.) Moreover, it has been suggested in Ref. 21 (among others) that the plane of "cyclic cleavage" is the slip plane, $\{10\bar{1}0\}_\alpha$ in the present instance, when the material has a planar slip character. If this interpretation is assumed, then Observation 5 may imply that cross slip occurs in the reversed plastic zone.

DISCUSSION

Influence of Texture

It is well known that crystallographic texture can significantly influence the mechanical properties of titanium alloys [30], including fatigue crack-growth rates [31-34]. One way to account for the influence of preferred orientation, at least in part, is through the elastic (Young's) modulus E [30,32]. In particular, it has been observed in several instances that growth rates can be normalized with respect to E; in other words, if ΔK were replaced by $\Delta K/E$ in Eq. (1),

$$da/dN = C'(\Delta K/E)^m , \tag{5}$$

the crack-growth rate curves would be expected to converge [2]. However in the present work, if such a normalization were undertaken by using the values of E in Table 1, the data plots for the MA and BA would in fact *diverge* from their present positions in Fig. 3. (Similar divergence was noted in the texture studies of Ref. 32.) Thus, on the basis of this test, the displacement between the MA and BA plots does not appear attributable to texture. That is not to say, however, that texture had no bearing on the present results (the nature of the structure-sensitive growth, etc.) or the differences between the present results and those of others.

Transitional Behavior

Among those differences, it is noted that the growth rate data for the BA in Ref. 6 did not exhibit a transition (and no mention of crack bifurcation was made), even though a fivefold enhancement in resistance was reported for the BA relative to the MA. The reason for this difference is unclear; it can be speculated, however, that if a larger $\bar{d}_{wp}$ were associated with the BA in Ref. 6 than in the present work, then a transitional r_y^c might not be attained until ΔK levels in excess of the largest reported in Ref. 6 (≈ 38 MPa $\cdot$ m$^{1/2}$) were reached.

It is further noted that the growth rate data for the BA in Ref. 7 *did* exhibit a transition, but at such low ΔK levels that r_y^c was reported to correlate with $\bar{d}_\alpha$ rather than $\bar{d}_{wp}$. ($\bar{d}_{wp}$ appears to be about an order of magnitude larger than $\bar{d}_\alpha$ in both the present work and Ref. 7.) The reason for this difference is unclear. It should be noted that structure-sensitive crack bifurcation was reported in Ref. 7 for crack growth below the transition.

Other instances of transitional behavior in Region 2 crack-growth data have been observed with Ti-6Al-4V alloys [29,35-37], for which detailed mechanisms could not be fully elucidated. It is interesting to note that Ref. 35 reports a transition in the case of

a MA. Moreover, as in the present work, crack branching was reported to occur below the transition.

Nature of the Structure-Sensitive Growth

The evidence in Fig. 5, as supported by the recent findings reported in Ref. 20, indicates that bifurcation in the present work does not occur along α/β interfaces, in contrast to the reports in Ref. 38 that enhanced propagation resistance in the case of a BA was attributable to α/β interface cracking. The reason for this apparent discrepancy is unclear; perhaps it is related to differences in texture or cooling rates. (It has recently been shown by Ref. 39 that the nature of the α/β interfacial phase, including crystal structure, can be radically affected by altering the cooling rate. Moreover, Ref. 40 recently reported some preliminary data to confirm the effect of cooling rate per se on da/dN for Ti-6Al-4V.)

Obviously, more work is needed to fully resolve the complex nature of structure-sensitive growth of fatigue cracks in Widmanstätten Ti-6Al-4V alloys.

SUMMARY

A beta anneal was found to significantly enhance the Region 2 fatigue crack propagation resistance of a commercial purity Ti-6Al-4V alloy, relative to the levels determined for a conventional mill anneal. Phenomenological highlights include the following:

1. The enhancement is particularly pronounced below a transition point in the crack-growth behavior of the beta-annealed material, which occurs at a stress-intensity factor range of $\Delta K = 23$ MPa$\cdot m^{1/2}$.

2. Below the transition point, growth rates are as much as an order of magnitude less for the beta anneal than determined for the mill anneal, although above the transition they are still at least a factor of three less.

3. In terms of the growth rate law, $da/dN = C(\Delta K)^m$, the exponent changes from $m \approx 3.1$ above the transition to $m \approx 6.3$ below.

Highlights from a micromechanistic interpretation of this behavior include the following:

1. It appears that the transition correlates with the point at which the reversed plastic zone attains the size of the relevant microstructural dimension (the Widmanstätten packet size).

2. In support of this interpretation, electron fractographic evidence indicates a change from microstructurally sensitive crack growth below the transition to insensitive above.

3. The role of the Widmanstätten packet in this structure-sensitive growth is revealed by metallographic crack-path sectioning. Within individual packets that border the

fracture surface, cracks appear at multiple parallel positions that bear a relation to the orientation of the α-phase platelets; i.e., these individual parallel platelets behave in unison, as a single crystal.

4. The transition, and the remarkably reduced growth rates that appear below it, are attributable to crack bifurcation, which serves to reduce the effective ΔK. As for the nature of the structure-sensitive crack growth, it was found that

- The fracture surface is faceted in appearance.
- The facets are comprised of three superposed features:

  River lines reminiscent of cleavage ("R-lines")

  Quilted lines which are of a configuration which resembles the Widmanstätten pattern of the microstructure ("W-lines"), and

  Very fine striations.

- The W-lines, which may be related to the origin of crack bifurcation, appear to trace slip bands (and ensuing slip-band cracks) as they cause offsets in the R-lines.

Other factors contributing to the enhancement associated with the β-anneal, exclusive of the transition, have been analyzed. These include the doubling of fracture toughness K_{I_c} from the level associated with the mill anneal, as well as fractographic distinctions. A commentary on the possible influence of texture is also included.

ACKNOWLEDGMENTS

The authors gratefully acknowledge the contributions of G. W. Jackson, M. L. Cigledy, C. R. Forsht, S. M. McCoy, and T. R. Harrison. Special thanks are also extended to P. F. Becher for help with scanning electron microscopy and to C. D. Beachem for a critical review of the manuscript. This work was supported by the Office of Naval Research.

REFERENCES

1. P. Paris and F. Erdogan, "A Critical Analysis of Crack Propagation Laws," *Trans. ASME, J. Basic Eng.* (Ser. D) 85, 528 (1963).
2. T. W. Crooker, "Designing Against Structural Failure Caused by Fatigue Crack Propagation," *Nav. Eng. J.* 84 (6), 46 (1972).
3. J. C. Chesnutt, C. G. Rhodes, and J. C. Williams, "The Relationship Between Mechanical Properties, Microstructure and Fracture Topography in α + β Titanium Alloys," in *Fractography—Microscopic Cracking Processes*, ASTM STP 600, American Society for Testing and Materials, Philadelphia, Pa., 1976, p. 99.

4. A Tobin, "The Role of Microstructure in Determining Fracture Toughness and Fatigue Properties of High Strength Titanium Alloys," Tech. Rep. RE-485, Grumman Aerospace Corporation, Bethpage, N.Y., Aug. 1974.

5. F. A. Crossley and R. E. Lewis, "Correlation of Microstructure with Fracture Toughness Properties in Metals," Lockheed Missiles and Space Company, Inc., Final Report on NASC Contract N00019-72-C-0545 (available from NTIS, Springfield, Va.), Sept. 1973, AD 772-103.

6. M. J. Harrigan, M. P. Kaplan, and A. W. Sommer, "Effect of Chemistry and Heat Treatment on the Fracture Properties of Ti-6Al-4V Alloy," in *Fracture Prevention and Control*, D. W. Hoeppner, ed., (Vol. 3 in the ASM Materials/Metalworking Technology Series), American Society for Metals, Metals Park, Ohio, 1974, p. 225.

7. P. E. Irving and C. J. Beevers, "Microstructural Influences on Fatigue Crack Growth in Ti-6Al-4V," *Mater. Sci. Eng.* 14, 229 (1974).

8. W. G. Clark, Jr., and S. J. Hudak, Jr., "Variability in Fatigue Crack Growth Rate Testing," *J. Testing and Evaluation* 3(6), 454 (1975).

9. E399-74, "Standard Method of Test for Plane-Strain Fracture Toughness of Metallic Materials," in *1975 Annual Book of ASTM Standards*, Part 10, American Society for Testing and Materials, Philadelphia, Pa., 1975, p. 561.

10. J. R. Rice, "Mechanics of Crack Tip Deformation and Extension by Fatigue," in *Fatigue Crack Propagation*, ASTM STP 415, American Society for Testing and Materials, Philadelphia, Pa., 1976, p. 247.

11. G. T. Hahn, R. G. Hoagland, and A. R. Rosenfield, "Local Yielding Attending Fatigue Crack Growth," *Met. Trans.* 3(5), 1189 (1972).

12. C. Bathias and R. M. Pelloux, "Fatigue Crack Propagation in Martensitic and Austenitic Steels," *Met. Trans.* 4(5), 1265 (1973).

13. R. Stevenson and J. F. Breedis, "Cyclic Deformation of Commercial-Purity Titanium," *Acta Metallurgica* 23(12), 1419 (1975).

14. R. K. Steele and A. J. McEvily, "The High-Cycle Fatigue Behavior of Ti-6Al-4V Alloy," *Eng. Fracture Mech.* 8(1), 31 (1976).

15. C. H. Wells and C. P. Sullivan, "Low-Cycle Fatigue Crack Initiation in Ti-6Al-4V," *ASM Trans. Quart.* 62(1), 263 (1969).

16. J. C. Williams, "Critical Review—Kinetics and Phase Transformations," *Titanium Science and Technology*, Vol. 3, R. I. Jaffee and H. M. Burte, eds., TMS-AIME, Plenum Press, New York, 1973, p. 1433.

17. W. G. Burgers, "On the Process of Transition of the Cubic-Body-Centered Modification into the Hexagonal-Close-Packed Modification of Zirconium," *Physica* 1, 561 (1934).

18. A. J. Williams, R. W. Cahn, and C. S. Barrett, "The Crystallography of the β-α Transformation in Titanium," *Acta Metallurgica* 2(1), 117 (1954).

19. P. A. Blenkinsop, Imperial Metal Industries (Kynoch) Limited, Birmingham, Great Britain, personal communication, Apr. 1976.

20. J. M. Barsom, "Fatigue-Crack Propagation in Steels of Various Yield Strengths, *Trans. ASME, J. Eng. Ind.* (Ser. B) 93(4), 1190 (1971).

21. A. Yuen, S. W. Hopkins, G. R. Leverant and C. A. Rau, "Correlations Between Fracture Surface Appearance and Fracture Mechanics Parameters for Stage II Fatigue Crack Propagation in Ti-6Al-4V," *Met. Trans.* 5(8), 1833 (1974)

22. C. J. Beevers, R. J. Cooke, J. F. Knott and R. O. Ritchie, "Some Considerations of the Influence of Sub-Critical Cleavage Growth During Fatigue-Crack Propagation in Steels," *Metal Sci.* 9, 119 (1975).

23. J. F. Knott, *Fundamentals of Fracture Mechanics*, Halsted Press, John Wiley and Sons, Inc., New York, 1973, pp. 251-256.

24. R. O. Ritchie and J. F. Knott, "Micro Cleavage Cracking During Fatigue Crack Propagation in Low Strength Steel," *Mater. Sci. Eng.* 14(1), 7 (1974).

25. G. H. Rowe, "Correlation of High-Cycle Fatigue Strength with True Stress-True Strain Behavior," *J. Mater.* 1(3), 689 (1966).

26. R. W. Hertzberg and W. J. Mills, "On the Character of Fatigue Fracture Surface Micromorphology in the Ultra-Low Growth Rate Regime," in *Fractography—Microscopic Cracking Processes*, ASTM STP 600, American Society for Testing and Materials, Philadelphia, Pa., 1976, p. 220.

27. C. D. Beachem and D. A. Meyn, "Fracture by Microscopic Plastic Deformation Processes," in *Electron Fractography*, ASTM STP 436, American Society for Testing and Materials, 1968, p. 59.

28. J. C. Williams, "Some Observations on the Stress-Corrosion Cracking of Three Commercial Titanium Alloys," *ASM Trans. Quart.* 60(4), 646 (1967).

29. D. A. Meyn, "An Analysis of Frequency and Amplitude Effects on Corrosion Fatigue Crack Propagation in Ti-8Al-1Mo-1V," *Met. Trans.* 2(3), 853 (1971).

30. F. Larson and A. Zarkades, "Properties of Textured Titanium Alloys," Rep. No. MCIC-74-20, Metals and Ceramics Information Center, Battelle-Columbus Laboratories (available from NTIS, AD 781884), June 1974.

31. R. J. H. Wanhill, "Environmental Fatigue Crack Propagation in Medium Strength Titanium Sheet Alloys," *Eng. Fracture Mech.* 6, 681 (1974).

32. M. J. Harrigan, A. W. Sommer, P. G. Reimers and G. A. Alers, "The Effect of Rolling Texture on the Fracture Mechanics Properties of Ti-6Al-2Sn-4Zr-6Mo Alloy," in Vol. 2, *Titanium Science and Technology*, Vol. 2, R. I. Jaffee and H. M. Burte, eds., TMS-AIME, Plenum Press, New York, 1973, p. 1297.

33. A. W. Bowen, "The Influence of Crystallographic Orientation on Fatigue Crack Growth in Strongly Textured Ti-6Al-4V," *Acta Metallurgica* 23(11), 1401 (1975).

34. C. A. Stubbington, "Metallurgical Aspects of Fatigue and Fracture in Titanium Alloys," in *AGARD Conference Proceedings No. 185, Specialists Meeting on Alloy Design for Fatigue and Fracture Resistance, 40th Meeting of the Structures and Materials Panel in Brussels, Belgium, Apr. 13-19, 1975*, p. 3-1, Advisory Group for Aerospace Research and Development (NATO), (available through NTIS as AGARD-CP-185).

35. R. P. Wei and D. L. Ritter, "The Influence of Temperature on Fatigue Crack Growth in a Mill Annealed Ti-6Al-4V Alloy," *J. Mater.* 7(2), 240 (1972).

36. R. L. Tobler, "Fatigue Crack Growth and J-Integral Fracture Parameters of Ti-6Al-4V at Ambient and Cryogenic Temperatures," in *Cracks and Fracture*, ASTM STP 601, American Society for Testing and Materials, Philadelphia, Pa., 1976, p. 346.

37. D. Eylon and C. M. Pierce, "Effect of Microstructure on Notch Fatigue Properties of Ti-6Al-4V," *Met. Trans.* 7A(1), 111 (1976).

38. N. E. Paton, J. C. Williams, J. C. Chesnutt and A. W. Thompson, "The Effects of Microstructure on the Fatigue and Fracture of Commercial Titanium Alloys," in *AGARD Conference Proceedings 185*, Jan. 1976, p. 4-1 (available through NTIS as AGARD-CP-185).

39. C. G. Rhodes and J. C. Williams, "Observations of an Interface Phase in the α/β Boundaries in Titanium Alloys," *Met. Trans.* 6A(8), 1670 (1975).

40. R. E. Lewis and F. A. Crossley, "Co elation of Microstructure With Fracture Toughness Properties in Metals (Part II)," Lockheed Missiles and Space Company, Inc., Report LMSC-D454884, Final Report for Period Nov. 21, 1973-Jan. 21, 1975, NASC Contract No. N00019-74-C-0161, Jan. 21, 1975.

*U S GOVERNMENT PRINTING OFFICE 19'6 240-824/043 1-3